

POLITECNICO DI MILANO

Scuola di Ingegneria Industriale e dell'Informazione
Corso di Laurea Magistrale in Automation and Control Engineering



POLITECNICO
MILANO 1863

Robot Assisted Minimally Invasive Surgery- Performance Analysis

Supervisor:
Prof. Luca Bascetta

Co- Supervisor:
Prof. Elena De Momi

Tesi di Laurea di:
Jagadesh Manivannan
Matricola:872291

Anno Accademico 2018/2019

Sommario

Questa tesi confronta le caratteristiche di prestazione di due controllori per un robot 7- GdL (Gradi di libertà) utilizzato per la chirurgia mini-invasiva assistita da robot (RAMIS). Questa tecnica garantisce il soddisfacimento di un vincolo chiamato "Remote Center of Motion" (RCM). Sono stati implementati due controller chiamati Cartesian Compliance Controller (CCC) e Adaptive Fuzzy Controller (AFC). Sono stati eseguiti esperimenti con compiti chirurgici virtuali, in un ambiente di realtà aumentata. Per validare la strategia di controllo proposta, sono stati eseguiti esperimenti con il robot KUKA LWR4+ in cui il robot ha seguito autonomamente il percorso relativo ad una attività in realtà virtuale generata online. I risultati ottenuti sono stati analizzati con i metodi Analysis of Variance (ANOVA) e Kruskal-Wallis, sono stati inoltre eseguiti vari test, basati sulla distribuzione normale, dei dati ottenuti con lo Statistics and Machine Learning Toolbox di MATLAB. I risultati dimostrano che l'accuratezza dell'end-effector finale e il vincolo RCM possono essere garantiti, riducendo quindi l'errore di posizione cartesiano e l'errore di restrizione RCM. Oltre a questo, i risultati Kruskal-Wallis dimostrano anche che il controller CCC è influenzato dal compito virtuale in modo più evidente mentre l'AFC è meno influenzato dalle attività virtuali, migliorando così le sue prestazioni. I risultati di ANOVA e Kruskal-Wallis riportano anche che l'errore di posizione cartesiano e l'errore di restrizione RCM sono stati tutti ridotti nell'AFC rispetto al CCC, dimostrando così che l'AFC ha caratteristiche di prestazioni più elevate rispetto a CCC.

Abstract

This thesis compares the performance of two controllers for a **7-DoF (Degree of Freedom) robot** used for robot assisted minimally invasive surgery (RAMIS). This guarantees a constraint called “**Remote Center of Motion**” (RCM). Two controllers called **Cartesian Compliance Controller (CCC)** and **Adaptive Fuzzy Controller (AFC)** are implemented and experiments with virtual surgical tasks, in an augmented reality environment are performed. The robot followed the path **autonomously over a virtual reality task** that is generated online, to verify and validate the proposed control strategy using **the KUKA LWR4+ robot**. The obtained results are analyzed with the **Analysis of Variance (ANOVA)** and **Kruskal-Wallis** tools and further followed by several tests based on the normality distribution of the obtained data using **MATLAB,2018a (Statistics and Machine Learning Toolbox)**. The results demonstrate that the end-effector’s accuracy as well as RCM constraint can be guaranteed, thereby reducing the Cartesian positional error and the RCM constraint error. In addition to this, Kruskal-Wallis results also prove that the CCC controller being influenced by the virtual task to a greater significance while the AFC being less influenced by the virtual tasks, thereby making its performance better. The results of ANOVA and Kruskal-Wallis also report that the Cartesian positional error and RCM constraint error were all reduced in the AFC compared to the CCC, thus making **AFC with higher performance characteristics than CCC**.

Contents

Sommario	3
Abstract	5
Introduction.....	12
CHAPTER 1	15
MATHEMATICAL TOOLS FOR STATISTICAL ANALYSIS	15
Benefits of ANOVA.....	16
Null Hypothesis.....	16
Confidence Intervals	17
Types of Error	19
Types of ANOVA	19
Assumptions of ANOVA	20
Analyzing and Evaluating the results of One-way ANOVA.....	20
Post-Hoc Test.....	21
Types of post-hoc tests	21
ANOVA Table	21
Drawing Conclusion based on results	23
Kruskal-Wallis Test.....	24
Assumptions of Kruskal-Wallis.....	24
Kruskal-Wallis Table.....	25
Drawing Conclusion based on results	26
Goodness of Fit Tests.....	27
Kolmogorov-Smirnov Test.....	27
Lilliefors (LF) Test	28
Homogeneity of Variance Tests	29
Levene Test.....	29
Bartlett Test.....	30

Chapter 2	31
Robotic Application- Minimally Invasive Surgery (MIS)	31
State of the Art- System Description.....	31
Design phases and Execution steps.....	32
RCM Constraint.....	32
Virtual trajectory tasks generation	34
Cartesian Compliance Controller (CCC)	36
Adaptive Fuzzy Controller (AFC).....	38
Chapter 3	39
Statistical Analysis of Experimental Results	39
Experimental Validation.....	39
Data Grouping	40
Similarity of two curves using Fréchet Distance.....	42
Statistical Analysis-Case1	42
Normality Check	42
Kruskal-Wallis Test for Cartesian Positional Error Analysis.....	43
Comparison among tasks in CCC controller	47
Comparison among tasks in AFC controller.....	49
Statistical Analysis-Case2	51
Data Grouping	51
Normality Check	53
Kruskal-Wallis Test for Remote Center of Motion (RCM) Error Analysis	54
Comparison among tasks in CCC controller	56
Comparison among tasks in AFC controller.....	58
Chapter 4	61
Discussion and Conclusion	61
References	63

List of Figures

Figure 1. Confidence Interval of 68%, 95%, 99%	18
Figure 2. Confidence Interval showing p-values	18
Figure 3. Type of Errors among groups	19
Figure 4. Overview of the robot assisted MIS system	31
Figure 5. RCM constraint: during surgery, the tool-tip must pass through the trocar position P_t , representing the RCM constraint. X and X_r are the actual and desired Cartesian position inside the abdomen	33
Figure 6. Task redundancy utilized to enforce RCM constraint (the grey and black "wrist" positions represent the desired, N_1d , and actual N , positions, respectively)	33
Figure 7. Task 1 representing a half-ellipsoidal wave	35
Figure 8. Task 2 representing a sine wave	36
Figure 9. Task 3 representing a triangular wave	36
Figure 10. Block diagram of Overall System with two controllers (CCC & AFC)	38
Figure 11. Desired Cartesian position by following three different task shapes for CCC	40
Figure 12. Enlarged image of x-axis with series of three different tasks for CCC ..	40
Figure 13. Actual Cartesian position by following three different task shapes for CCC	41
Figure 14. Enlarged image of x-axis with series of three different tasks for CCC ...	41
Figure 15. Non-normally distributed data for Cartesian positional error	43
Figure 16. Box-plot for three different tasks with two controllers	44
Figure 17. Significant Difference between CCC and AFC for task 1	46
Figure 18. Significant Difference between CCC and AFC for task 2	46
Figure 19. Significant Difference between CCC and AFC for task 3	46
Figure 20. Box-plot of three different tasks for CCC controller	47
Figure 21. Box-plot of three different tasks for AFC controller	49
Figure 22. RCM Error by following three different task shapes for CCC	52
Figure 23. Enlarged image with series of three different tasks for CCC	53
Figure 24. Non-normal distribution of data for RCM error	53
Figure 25. Box-plot of three different tasks for RCM error	54
Figure 26. Box-plot of three different tasks for CCC controller	56
Figure 27. Box-plot of three different tasks for AFC controller	58

List of Tables

Table 1. Available methods and tools of Data Analysis	13
Table 2. Two Processes to execute based on results of the assumptions check...	15
Table 3. Significance Table displaying significance type for different p-values.....	18
Table 4. ANOVA table with formulas of the parameters	21
Table 5. Kruskal-Wallis table with formulas of the parameters.....	25
Table 6. Experimental grouping of Data.....	39
Table 7. Task1 significant difference among controllers	44
Table 8. Task2 significant difference among controllers	45
Table 9. Task3 significant difference among controllers	45
Table 10. Task1 and 2 comparison using CCC controller	48
Table 11. Task2 and 3 comparison using CCC controller	48
Table 12. Task1 and 3 comparison using CCC controller	48
Table 13. Task1 and 2 comparison using AFC controller	50
Table 14. Task2 and 3 comparison using AFC controller	50
Table 15. Task1 and 3 comparison using AFC controller	50
Table 16. Task1 and 2 comparison using AFC controller-ANOVA (False Positive) ..	51
Table 17. Task1 significant difference among controllers	55
Table 18. Task2 significant difference among controllers	55
Table 19. Task3 significant difference among controllers	55
Table 20. Task1 and 2 comparison using CCC controller	57
Table 21. Task2 and 3 comparison using CCC controller	57
Table 22. Task1 and 3 comparison using CCC controller	57
Table 23. Task1 and 2 comparison using AFC controller	59
Table 24. Task2 and 3 comparison using AFC controller	59
Table 25. Task1 and 3 comparison using AFC controller	59

Introduction

Robot-assisted surgery has been more popular over the recent years for the advantages it can offer, like greater surgical precision, increased range of motion, improved dexterity and enhanced visualization for surgeons [1]. In the traditional Minimally Invasive Surgery, the surgical tip must go through small incisions on the patient's abdominal wall. Each small incision produces a kinematic constraint, commonly known as the **Remote Center of Motion (RCM)** constraint [2], [3]. In general, the RCM constraint can be active or passive, where the passive constraint is maintained mechanically, while the active method is known to be achieved with a software controller [4], [5] and is more popular in the non-clinical research, since it is cost-less and provides a flexible task space.

A **Cartesian Compliance Controller (CCC)** and an **Adaptive Fuzzy Controller (AFC)** was implemented as in [6]. The two controllers' performance with respect to the RCM constraint error and Cartesian positional error are compared with various techniques available for data analysis.

A collection of statistical models and their associated estimation procedures (such as variation among and between groups) were used to analyze the differences among group means in a sample. Several methods like **Analysis of variance (ANOVA)**, **Kruskal-Wallis** were in existence from 20th century [7]. Randomization models were developed by several researchers as in [8], [9], [10]. ANOVA ensures computational elegance, and this made it so popular in the mathematics and statistical society; Kruskal-Wallis is more preferred than ANOVA especially in cases where the distribution of samples are not normally distributed. Kruskal-Wallis performs the non- parametric one-way ANOVA for non-normally distributed data [11], [12], [13]. The significant differences among the specific groups can be calculated using **Mann-Whitney U test**, **Tukey's post-hoc test**, **Bonferroni test**, **Dunn's test**, etc. [14], [15]. Some of the available tools for data analysis is reported in Table 1.

Type of Test	Use
Correlational	These tests look for an association between variables
Pearson correlation	Tests for the strength of the association between two continuous variables
Spearman correlation	Tests for the strength of the association between two ordinal variables (does not rely on the assumption of normally distributed data)
Chi-square	Tests for the strength of the association between two categorical variables
Comparison of Means: look for the difference between the means of variables	
Paired T-test	Tests for the difference between two related variables
Independent T-test	Tests for the difference between two independent variables
ANOVA	Tests the difference between group means after any other variance in the outcome variable is accounted for
Regression: assess if change in one variable predicts change in another variable	
Simple regression	Tests how change in the predictor variable predicts the level of change in the outcome variable
Multiple regression	Tests how change in the combination of two or more predictor variables predict the level of change in the outcome variable
Non-parametric: used when the data does not meet assumptions required for parametric tests	
Kruskal-Wallis test	Test for the difference between group means performing one-way ANOVA
Wilcoxon rank-sum test	Tests for the difference between two independent variables—takes into account magnitude and direction of difference
Wilcoxon sign-rank test	Tests for the difference between two related variables—takes into account the magnitude and direction of difference
Sign test	Tests if two related variables are different—ignores the magnitude of change, only takes into account direction

Table 1. Available methods and tools of Data Analysis

Analyzing engineering results using statistical methods helps to a great extent to validate and verify whether the results were satisfying the expectations of the engineers and how well it performed with respect to certain parameters.

Finally, experiments using a 7-DoF serial robot KUKA LWR4+ and considering a virtual surgical task tracking have been performed; the obtained data was validated using the above-mentioned methods of data analysis to validate the performance characteristics among the two controllers (CCC & AFC).

This thesis report is organized as follows. CHAPTER 1 describes the mathematical tools available for statistical analysis, explains the goodness of fit test available to check the normality distribution, describes the homogeneity of variance tests to be fulfilled. Chapter 2 describes about a robotic application that is used to perform Robot Assisted Minimally Invasive Surgery (RAMIS) with different control strategies to achieve Remote Center of Motion (RCM) constraint with the control equations and block diagrams. The complete data analysis with the obtained results (data) from the robotic application has been reported in Chapter 3. Finally, the conclusions are reported in Chapter 4.

CHAPTER 1

MATHEMATICAL TOOLS FOR STATISTICAL ANALYSIS

After performing experiments, it is always important and much better to analyze the data obtained in order to compare them, to analyze the differences and to arrive at conclusions. There are several mathematical tools available to carry out the statistical analysis as shown in Table 1 based on the requirements. This Chapter describes the most widely used mathematical tools and statistical analysis techniques whose final aim is to verify and validate the correctness of the result obtained with the experimental data. The two most reliable tools explained below are ANOVA test and Kruskal-Wallis test. There are certain assumptions that has to be checked/satisfied in order to proceed with both the tests. The chapter consists of two main statistical tests (ANOVA and Kruskal-Wallis) and other tests to check the assumptions of the two tests mentioned before. For instance, if we have some data and we would like to do a statistical analysis, the following table is useful to proceed:

Process I (ANOVA)	Process II (Kruskal-Wallis)
Normally distributed data (Kolmogorov-Smirnov test)	Non-Normally distributed data (Lilliefors test)
Equal variance of data (Bartlett test)	Equal variance of data (Levene's Test)

Table 2. Two Processes to execute based on results of the assumptions check

If the data is normally distributed (checked by Kolmogorov-Smirnov test), then we should proceed with Bartlett test and then the data can be processed using ANOVA. If the data is not normally distributed (checked by Lilliefors test), then we should proceed with Levene's test and then the data can be processed using Kruskal-Wallis.

ANOVA

The best way to compare two or more groups of data is to use the ANOVA (**Analysis Of VAriance**) test. In addition to the above tools, there are more tests like hypothesis testing, partitioning of sum of squares, additive models. ANOVA was founded by Sir Ronald Fisher in 1925 [7], [16] . It is easy to be computed manually using simple algebra rather than complex matrices. This was one of the main reason for the popularity of using ANOVA over other tools.

Benefits of ANOVA

Analysis of variance is a group of statistical tool to test if there exists a significant difference between the means of various groups. When there are only two samples, T-test and ANOVA yields the same results. In cases of more than two samples, ANOVA is the most effective to compare the means. Hence ANOVA is one of the widely used tool in research for validating the experimental data statistically. Another advantage of ANOVA is that it can be used effectively even when the number of observations is different in each group.

Null Hypothesis

ANOVA tests the non-specific null hypothesis that all populated means are equal.

$$\begin{aligned} H_0: \mu_1 &= \mu_2 = \mu_3 = \dots = \mu_k \\ H_1: \mu_1 &\neq \mu_2 \neq \mu_3 \neq \dots \neq \mu_k \end{aligned} \tag{1}$$

ANOVA generates a P value (probability) for the null hypothesis (H_0) and thus a probability for the research hypothesis (H_1) to be tested. The lower the p value, the smaller the probability for the null hypothesis to be true and consequently higher is the probability that there is a significant statistical difference between the data sets (or the research hypothesis H_1 is true).

Confidence Intervals

Confidence interval is a type of interval estimate computed from the statistics of the observed data, that might contain the true value of an unknown population parameter. The selection of a confidence level for an interval determines the probability that the confidence interval produced will contain the true parameter value. Common choices for the confidence level are 0.90, 0.95, and 0.99. These levels correspond to percentages of the area of the normal density curve. For example, a 95% confidence interval covers 95% of the normal curve - the probability of observing a value outside of this area is less than 0.05 (which is called '**alpha**'). Because the normal curve is symmetric, half of the area is in the left tail of the curve, and the other half of the area is in the right tail of the curve and the peak represents the mean value of the distribution. Figure 1 displays the confidence intervals of 68%, 95% and 99%. Figure 2 represents the p-values (0.05,0.01,0.10) which are tested during the null hypothesis for 95%,99% and 90% confidence interval. There is also a z-score corresponding to each p-value which is nothing but a value from the standard normal distribution for the selected confidence level. The null hypothesis is usually tested for various significance levels (0.05,0.01,0.10). By default, the significance level of testing is set to 0.05 in most of the tests. This signifies that the means of the data being tested lies in the 95% of the confidence region and the rest 5% are prone to errors. If the null hypothesis is rejected, it means that the data among various groups compared have a significant difference which does not fall under the confidence interval. In any test, this significance level can be altered for the level which we would like to compare, and then the null hypothesis can be checked. Table 3 displays the significance table showing the p-values and their significance level during the analysis of data.

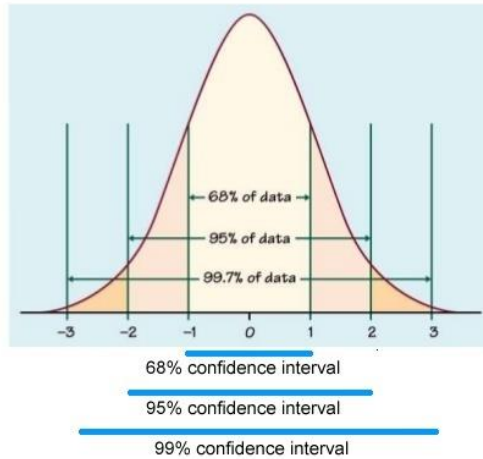


Figure 1. Confidence Interval of 68%, 95%, 99%

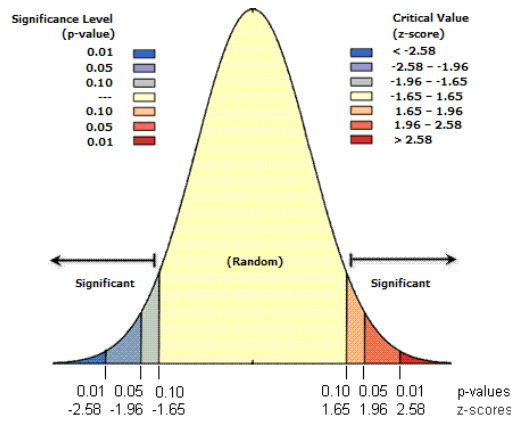


Figure 2. Confidence Interval showing p-values

Significance Value (p-val)	Significance Type
$p < 0.05 (*)$	Significant Difference (confidence interval 95%)
$p < 0.01 (**)$	Significant Difference (confidence interval 99%)
$p < 0.001 (***)$	Very-High Significant Difference

Table 3. Significance Table displaying significance type for different p-values

Types of Error

There are two types of error that can occur if ANOVA is executed in a wrong way:

- Type I Error (α error or false positive): Error of finding a significance by chance when there is no significance in the data.
- Type II Error (β error or false negative): Error of rejecting a significance when in fact there is a significance in the data.

Figure 3 represents the two types of errors that can happen when checking for a null hypothesis using ANOVA or any other methods.

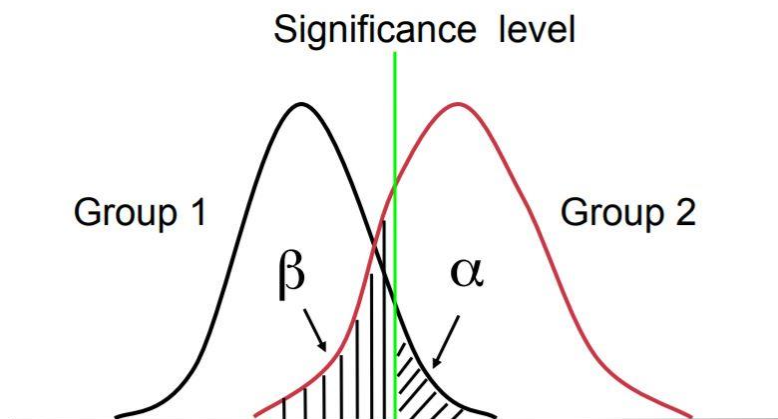


Figure 3. Type of Errors among groups

Types of ANOVA

- *One-way ANOVA*: One-way ANOVA is a hypothesis test, used to test the equality of three or more groups of data means simultaneously using variance (just one independent variable). The number of data in each group need not to be equal.
- *Two-way ANOVA*: Two-way ANOVA is a statistical technique wherein, the interaction between factors, influencing variable can be studied (i.e. groups with more two independent variables). The number of data in each group needs to be equal.

- *N-way ANOVA*: N-way ANOVA is the extended process of the two-way ANOVA where there are n-independent variables. The evaluation procedure remains same.

Assumptions of ANOVA

Before starting to continue the data processing with ANOVA, it is necessary to meet or fulfill the assumptions of ANOVA:

- The data from all the groups are normally distributed.
- The data from all the groups have almost equal variances.
- The data obtained are independent.

ANOVA is **robust** to some violations (mild) of its assumptions and it is conservative. Though the ANOVA is robust, it is better to check for the above-mentioned assumptions of ANOVA. If the assumptions are not met, the data can be either processed to meet the assumptions or to switch to non-parametric test like Kruskal-Wallis (which does not require any data normalization).

Analyzing and Evaluating the results of One-way ANOVA

The output of a one-way ANOVA contains the significance value (p) which determines the amount of difference by which a group of data significantly differs from another group of data. The tolerance value (represented by α) is set to 0.05 by default.

- **$p > \alpha$** : If the p value is greater than α , it is considered that there is no statistically significant difference between the group means as determined by the one-way ANOVA; for this reason, there is no need for a post-hoc test.
- **$p < \alpha$** : If the p value is lesser than α , it is considered that there is a significant difference between the group means as determined by the one-way ANOVA; which is always followed by a post-hoc test.

Post-Hoc Test

The results of an ANOVA test provide only the overall difference between the groups and doesn't provide any precise information about which specific group differed from another, but post-hoc tests do. The post-hoc test is nothing but a follow-up test that is run to confirm whether the differences among the groups show an overall statistically significant difference in the groups' mean.

Types of post-hoc tests

- Tukey's honestly significant difference criterion ('hsd' or 'tukey-kramer')
- Tukey's least significant difference procedure ('lsd')
- Bonferroni adjustment ('bonferroni')
- Dunn-Sidak procedure ('dunn-sidak')
- Scheffé's S procedure ('scheffe')

If the data has met the assumptions homogeneity of variances, it is always better to use the Tukey's honestly significant difference post-hoc method over the other above-proposed methods. If not, it is advisable to run the Games Howell post hoc test.

ANOVA Table

Source	SS	df	MS	F	p
Model/Group	SSG	$k - 1$	$MSG = \frac{SSG}{k - 1}$	$\frac{MSG}{MSE}$	
Residual/Error	SSE	$n - k$	$MSE = \frac{SSE}{n - k}$		
Total	SST	$n - 1$			

Table 4. ANOVA table with formulas of the parameters

The following are the key symbols that will be used henceforth:

k = number of groups/ populations/ values of the explanatory variable/ levels of treatment

n_i = the sample size taken from group i

x_{ij} = the j^{th} response sampled from the i^{th} group/ population

\bar{x}_i = the sample mean of responses from the i^{th} group = $\frac{1}{n_i} \sum_{j=1}^{n_i} x_{ij}$

s_i = the sample standard deviation from the i^{th} group = $\frac{1}{n_i-1} \sum_{j=1}^{n_i} (x_{ij} - \bar{x}_i)^2$

n = the (total) sample, irrespective of groups = $\sum_{i=1}^k n_i$

\bar{x} = the mean of all responses, irrespective of groups = $\frac{1}{n} \sum_{ij} x_{ij}$

Each and every column of the table is explained below as follows. The source (of variability) row tell us:

- SS: Sum of squares (sum of squared deviations) which contains:
 - SST (sum of squares total) measures the variation of data around the overall mean \bar{x} . It can be calculated as:

$$\sum_{i=1}^k \sum_{j=1}^{n_i} (x_{ij} - \bar{x})^2 \quad (2)$$

- SSG measures variation of the group means around the overall mean \bar{x} . Variability between the group means is given by:

$$\sum_{i=1}^k n_i (\bar{x}_i - \bar{x})^2 \quad \text{and} \quad (3)$$

- SSE measures the variation of each observation around its group mean \bar{x}_i . Variability within the group means is given by:

$$\sum_{i=1}^k \sum_{j=1}^{n_i} (x_{ij} - \bar{x}_i)^2 = \sum_{i=1}^k (n_i - 1) s_i^2 \quad (4)$$

$$SST = SSG + SSE \quad (5)$$

- Df represents the degree of freedom. The degrees of freedom are given as:
 - $k - 1$ for SSG, since it measures the variation of the k group means about the overall mean.
 - $n - k$ for SSE, since it measures the variation of the n observations about the overall mean.
- MS represents the mean square which is already given in the ANOVA table above. In addition to that, mean square can also be calculated as:

$$MSE = \frac{(n_1 - 1)s_1^2 + (n_2 - 1)s_2^2 + \dots + (n_k - 1)s_k^2}{(n_1 - 1) + (n_2 - 1) + \dots + (n_k - 1)} \quad (6)$$

- The final column of the ANOVA table is the F statistic which is given by:

$$F \text{ statistic} = \frac{MSG}{MSE} \quad (7)$$

If the null hypothesis is true, the F statistic has an F distribution with $k - 1$ and $n - k$ degrees of freedom in the numerator/denominator respectively. If the alternate hypothesis is true, then F tends to be large. We reject H_0 in favor of H_1 if the F statistic is sufficiently large.

The final column in the ANOVA table consists of the significance value which yields the result (to accept the null hypothesis or not).

Drawing Conclusion based on results

The ANOVA's results are used to draw conclusions based on the validations and tests performed on the datasets. It is very important to compare different methods and find which method is best suited for the aim of the experiment for which the data was obtained. ANOVA also helps in finding which method has a better performance characteristics based on experiment-specific criteria. As a result, the obtained data becomes not only experimentally correct, but also statistically valid. The ANOVA exploits the data among the groups to analyze the significant differences and results can be checked further about the cause of the significant differences among the groups.

Kruskal-Wallis Test

The Kruskal-Wallis test (named after William Kruskal and W. Allen Wallis) is a rank based non-parametric method for testing ANOVA [11], [17]. It is a multiple-sample generalization of the two-sample Wilcoxon rank sum test [18]. It determines the statistical significances between two or more groups of an independent variable on a continuous or ordinal dependent variable. It is important to realize that the Kruskal-Wallis H test is an *omnibus* test statistic and cannot tell which specific groups of the independent variable are statistically significantly different from each other; it only tells that at least two groups were different. The greatest advantage of Kruskal-Wallis is that it returns the exact probability values for larger sample sizes [19].

Assumptions of Kruskal-Wallis

Though the Kruskal-Wallis is a replacement of ANOVA when the data is not normally distributed, it still has some assumption to be checked before proceeding with the test. The assumptions of ANOVA are as follows:

- The data should be measured at a continuous level.
- The independent variable should consist two or more categorical independent groups.
- The data obtained should have independence of observations, which means that there is no relationship between the observations in each group or between the groups.
- In order to know how to interpret the results from a Kruskal-Wallis test, it is quite good to determine whether the distributions in each group are the same (i.e. having the same shape). This is a non-necessary condition for the test.

Kruskal-Wallis Table

Source	SS	df	MS	Chi-sq	Prob>Chi-sq
Model/Group	SSG	$k - 1$	$MSG = \frac{SSG}{k - 1}$		
Residual/Error	SSE	$n - k$	$MSE = \frac{SSE}{n - k}$		
Total	SST	$n - 1$			

Table 5. Kruskal-Wallis table with formulas of the parameters

The Kruskal-Wallis table is almost similar to the ANOVA table and its formulas are mostly same except for the Chi-sq. Samples of sizes $n_j, j = 1, \dots, k$, are combined and ranked in ascending order of magnitude. Tied values are assigned the average ranks. If n represent the overall sample size, and the sum of ranks for the j^{th} sample is given by:

$$R_j = \sum_{i=1}^{n_j} R(x_{ij}) \quad (8)$$

where,

x_{ij} = the j^{th} response sampled from the i^{th} group/ population.

The Kruskal-Wallis one-way analysis of variance test, H is defined as:

$$H = \frac{1}{s^2} \left\{ \sum_{j=1}^m \frac{R_j^2}{n_j} - \frac{n(n+1)^2}{4} \right\} \quad (9)$$

where

$$s^2 = \frac{1}{n-1} \left\{ \sum_{\text{all ranks}} R(x_{ij})^2 - \frac{n(n+1)^2}{4} \right\} \quad (10)$$

If there are no ties, the equation simplifies to

$$H = \frac{12}{n(n+1)} \sum_{j=1}^m \frac{R_j^2}{n_j} - 3(n+1) \quad (11)$$

In case of a tie, a correction for tie is implemented using the short cut formula:

$$\text{Correction} = \frac{H}{1 - \frac{\sum_{i=1}^G (t_i^3 - t_i)}{n^3 - n}} \quad (12)$$

where G is the number of groupings of different tied ranks, and t_i is the number of tied values within group i that are tied at a particular value. The correction usually makes little difference in the value of H unless there are a large number of ties. The sampling of the distribution H is approximately Chi-square (χ^2) with $k - 1$ degrees of freedom.

Finally, the p-value is approximated by $Pr(\chi_{k-1}^2 \geq H)$. If some n_j values are small (i.e., less than 5), the probability distribution of H can be quite different from its chi-squared distribution. If a table of chi-squared probability distribution is available, the critical value of chi-squared, $\chi_{\alpha:k-1}^2$, can be found by entering the table at $k - 1$ degrees of freedom and looking under the desired significance or alpha level. The table of chi-squared probability distribution for $k = 1, 2, \dots, 1000$ degrees of freedom is reported in [20].

Drawing Conclusion based on results

The Kruskal-Wallis table is used to draw conclusions based on the validations and tests performed on the datasets. Though the Kruskal-Wallis does not say which groups are significantly different from each other, it gives a better result for the overall significant difference among all the groups (especially for non-normally distributed data).

Goodness of Fit Tests

In order to check and satisfy the assumptions of ANOVA, it is mandatory to check the distributions of the data in each group. The distributions can be any (e.g. 'normal', 'extreme value', 'exponential', etc.); but ANOVA processes the data at its best when the data is normally distributed. The data distribution can be checked mainly by the following two tests:

- Kolmogorov- Smirnov (KS) test.
- Lilliefors (LF) test.

Kolmogorov-Smirnov Test

The Kolmogorov-Smirnov test tests whether two arbitrary distributions are the same. It can be used to compare two empirical data distributions, or to compare one empirical data distribution to any reference distribution. It's based on comparing two cumulative distribution functions (CDFs). Remember that the CDF of a random variable x is the probability that the random variable is less than or equal to some value. To be a bit more precise, it's a function F such that

$$F(a) = P(x \leq a) \quad (13)$$

When talking about data, it's often useful to look at empirical CDFs:

$$F_n(a) = \frac{1}{n} \sum_i \mathbb{I}(x_i - a) \quad (14)$$

is the CDF of n observed data points; and \mathbb{I} is a function that returns 1 when its argument is true and 0 when its argument is false. Now suppose we want to compare two CDFs, F^1 and F^2 . They might be empirical CDFs (to compare two different datasets and see whether they're significantly different) or one might be a reference CDF (to see whether a particular distribution is an appropriate choice for a dataset). The Kolmogorov-Smirnov test computes the statistic h :

$$h = \max_x |F_n^1(x) - F_n^2(x)| \quad (15)$$

This compares the two CDFs and looks at the point of maximum discrepancy. We can theoretically show that if F^1 is the empirical distribution of x and F^2 is the

true distribution x was drawn from, then $\lim_{n \rightarrow \infty} h = 0$. Similarly, if the two distributions have no overlap at all, the maximum difference will be 1 (when one CDF is 1 and the other is 0). Therefore, we can test distribution equality by comparing the statistic h to 0 (if h is significantly larger than 0 and close to 1, then we might conclude that the distributions are not equal). This method is only defined for one-dimensional random variables: although there are extensions to multiple random variables; they are more complex than simply comparing joint CDFs. Also notice that this test is sensitive to any differences at all in two distributions: two distributions with the same mean but significantly different shapes will produce a large value of h .

Lilliefors (LF) Test

Lilliefors (LF) test is a modification of the Kolmogorov-Smirnov test. The KS test is appropriate in a situation where the parameters of the hypothesized distribution are completely known. However, sometimes it is difficult to initially or completely specify the parameters as the distribution is unknown. In this case, the parameters need to be estimated based on the sample data. When the original KS statistic is used in such situation, the results can be misleading whereby the probability of type I error tend to be smaller than the ones given in the standard table of the KS test. In contrast with the KS test, the parameters of the LF test are estimated based on the sample. Therefore, in this situation, the LF test will be preferred over the KS test. Given a sample of n observations, the LF statistic is defined as:

$$h = \max_x |F^*(x) - S_n(x)| \quad (16)$$

Where $S_n(x)$ is the sample cumulative distributive function and $F^*(x)$ is the cumulative normal distribution function with $\mu = \bar{x}$, the sample mean and σ^2 , the sample variance, defined with denominator $n - 1$. Even though the LF statistic is the same as the KS statistic, the table for the critical values is different which leads to a different conclusion about the normality of a data (Mendes & Pala, 2003). If h is significantly larger than 0 and close to 1, then we might conclude that the distributions are not equal and that it rejects the null hypothesis.

Homogeneity of Variance Tests

In order to check and satisfy the assumptions of ANOVA, it is mandatory to check the equality of variances of the data in each group. The variances of the data can be equal or not equal among the groups. The homogeneity of variances can be checked mainly by the following two tests:

- Levene test.
- Bartlett test.

Levene Test

Levene test is used to test whether two or more population variances are equal. The test does not assume that all populations are normally distributed and **is recommended when the normality assumption is not viable**. Suppose g groups each have a normal distribution with possibly different means and standard deviations $\sigma_1, \sigma_2, \dots, \sigma_g$. Let n_1, n_2, \dots, n_g denotes the number of subjects in each group, Y_{ki} denote the response values, and N denote the total sample size of all groups. The test assumes that the data are obtained by taking a simple random sample from each of the g populations. The formula for the calculation of Levene's test is

$$W = \frac{(N - g) \sum_{k=1}^g n_k (Z_k - \bar{Z})^2}{(g - 1) \left\{ \sum_{k=1}^g \sum_{i=1}^{n_k} n_k (Z_{ki} - \bar{Z}_k)^2 \right\}} \quad (17)$$

where

$$Z_{ki} = |Y_{ki} - \bar{Y}_k|$$

$$Z_k = \frac{1}{n_k} \sum_{i=1}^{n_k} Z_{ki}$$

$$\bar{Z} = \frac{1}{N} \sum_{k=1}^g \sum_{i=1}^{n_k} Z_{ki}$$

$$\bar{Y}_k = \frac{1}{n_k} \sum_{i=1}^{n_k} Y_{ki}$$

If the assumptions are met, the distribution of this test statistic follows the F distribution with degrees of freedom $g - 1$ and $N - g$.

Bartlett Test

Bartlett (1937) presents a test of homogeneity (equal variance). The test assumes that all populations are normally distributed and is **not recommended when the normality assumption is not viable**. Suppose g groups each have a normal distribution with possibly different means and standard deviations $\sigma_1, \sigma_2, \dots, \sigma_g$. Let n_1, n_2, \dots, n_g denotes the number of subjects in each group, and let N denote the total sample size of all groups. The test assumes that the data are obtained by taking a simple random sample from each of the g populations.

The formula for the calculation of Bartlett's test is:

$$\chi_{g-1}^2 = \frac{(N - g) \log(S_p^2) - \sum_{k=1}^g (n_k - 1) \log(S_k^2)}{1 + \frac{1}{3g - 3} \left\{ \sum_{k=1}^g \left(\frac{1}{n_k - 1} \right) - \frac{1}{N - g} \right\}} \quad (18)$$

where

$$S_p^2 = \frac{1}{N - g} \sum_{k=1}^g (n_k - 1) S_k^2$$

$$S_k^2 = \frac{1}{n_k - 1} \sum_{i=1}^{n_k} (x_{ki} - \bar{x}_k)^2$$

If the assumptions are met, the distribution of this test statistic follows the Chi-squared distribution with degrees of freedom $g - 1$.

Chapter 2

Robotic Application- Minimally Invasive Surgery (MIS)

This chapter explains the robotic system developed for autonomous MIS with its controllers implemented and tested successfully. It gives a brief explanation about the state of the art by explaining about the robotic manipulator, communication protocols, devices and the control methodology.

State of the Art- System Description

An overview of the developed robot assisted MIS system shown in Figure 4.

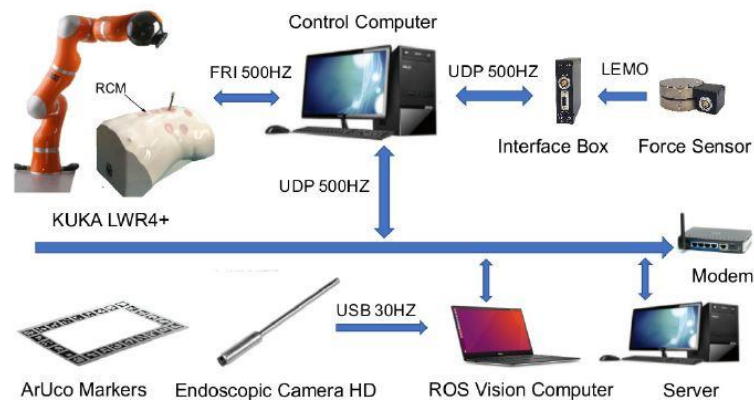


Figure 4. Overview of the robot assisted MIS system

The system is composed of:

- a KUKA LWR4+ redundant robot, that is torque-controlled through the Fast Research Interface (FRI), providing a direct low-level real-time access to the robot controller [21];
- an HD endoscopic camera and an ArUco marker board [22], that are used for virtual surgical task tracking in an augmented reality environment;
- a 6-axis M8128C6 force sensor, adopted to measure the interaction force between the surgical tip and the abdominal wall.

The control system has been developed using two separate computers communicating through an UDP channel. The first one, the “control computer”, executes the real-time control loops implemented using OROCOS, with a real-time Xenomai-patched Linux kernel. The second one, the “vision computer”, runs the perception algorithms developed using ROS Kinetic under Ubuntu.

Design phases and Execution steps

The design phase involves the following set-up procedures that has to be executed in order to test the robot with different subjects.

- RCM constraint;
- Virtual trajectory tasks generation;
- Cartesian Compliance Controller (CCC) and
- Adaptive Fuzzy Controller (AFC).

RCM Constraint

During Minimally Invasive Surgery (MIS), the surgical tool tip has to pass through small incisions on the patient’s abdominal wall. Each small incisions produces a kinematic constraint, commonly known as the Remote Center of Motion (RCM) constraint. In general, RCM constraint can be active or passive where the passive constraint can be achieved by mechanical designs and active constraints can be achieved by online controller design. There are pretty much of strategies proposed in the literature to achieve the active RCM constraint by taking advantage of the task redundancy.

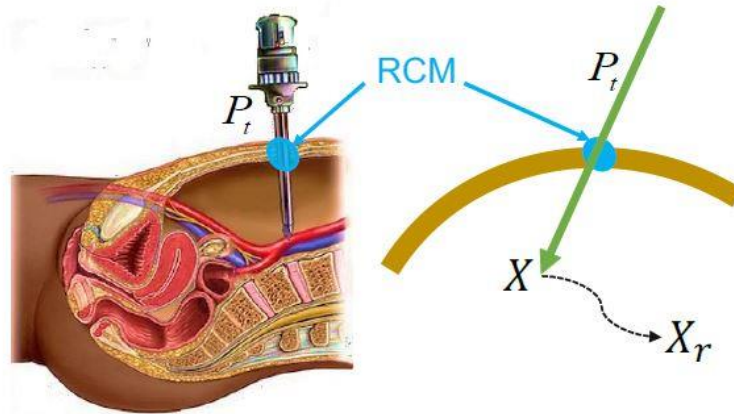


Figure 5. RCM constraint: during surgery, the tool-tip must pass through the trocar position P_t , representing the RCM constraint. X and X_r are the actual and desired Cartesian position inside the abdomen

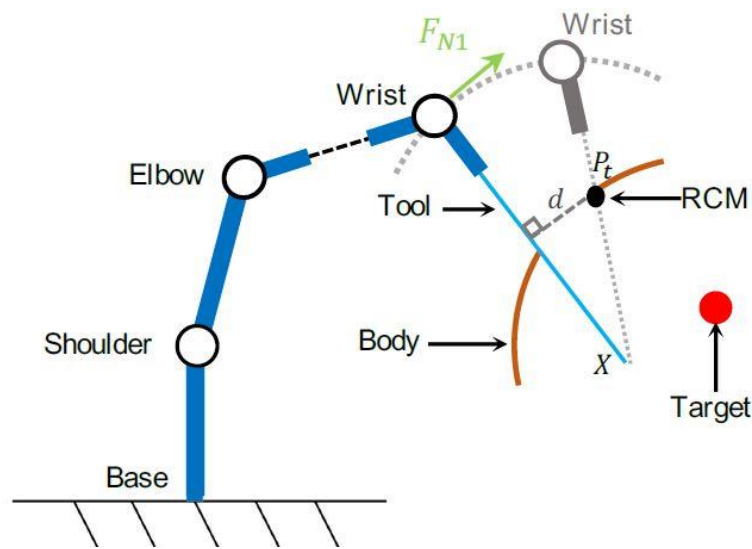


Figure 6. Task redundancy utilized to enforce RCM constraint (the grey and black "wrist" positions represent the desired, N_{1d} , and actual N_1 , positions, respectively)

During the auto-tracking of a surgical task, three out of the seven robot degrees of freedom are exploited, and the other four degrees of freedom remain as redundancy. Part of these redundant degree of freedom are used here by the first null-space controller to fulfil the RCM constraint. Figure 5 and Figure 6 shows the RCM constraint to guarantee the tool always enters the patient body through the trocar point P_t , without influencing the main surgical task, i.e., acting in the null space of the surgical task, the "wrist" joint has to track a circular movement around the end-effector from its actual position N_1 to the desired position N_{1d} .

A control action that enforces this constraint is thus given by:

$$F_{N1} = -K_{N1}e_{N1} - D_{N1}\dot{e}_{N1} \quad (19)$$

where $K_{N1}, D_{N1} \in \mathbb{R}^3$ are the stiffness and damping matrices respectively, and $e_{N1} = N1 - N_{1d}$ is the “wrist” tracking error. Projecting this action into the null-space of the surgical task, the first null-space controller can be introduced as:

$$\tau_{N1} = (I - J_T^T(q)J^T(q))J_W^T(q)F_{N1} \quad (20)$$

where $J_W(q) \in \mathbb{R}^{3 \times 5}$ is the Jacobian from the base frame to the robot wrist. Further, the distance (d in Figure 6) can be seen as:

$$d = \|(P_t - X) \times \hat{u}_c\| \quad (21)$$

where $\hat{u}_c \in \mathbb{R}^3$ is the actual tip direction vector. It can be easily shown that $\|e_{N1}\|$ is proportional to the RCM constraint error d , i.e., $d = \lambda\|e_{N1}\|, \lambda \in (0,1]$, where e_{N1} can be further expressed as

$$e_{N1} = \frac{\|(P_t - X) \times \hat{u}_c\|}{\lambda} \quad (22)$$

where P_t, X, \hat{u}_c are all known terms. In general, λ varies according to the tip position during the operation. But throughout the process, we choose λ as a constant.

Virtual trajectory tasks generation

It is important to design any virtual task before practically testing the robot on the real human patient. Hence, a virtual trajectory tasks very designed with the aid of an HD endoscopic camera and an ArUco marker board in an augmented reality environment. By creating this tasks, the robot can autonomously follow the path shown by the virtual trajectory to execute the task. Three different task shapes were designed: a half ellipsoidal wave, a sine wave and a triangular wave. The size of the designed tasks are around $8.0cm \times 15.0cm$ on the horizontal plane, which is similar to an actual laparoscopic surgical task. The vision interface displays the

camera images, the desired task path (in green color) and the actual paths (in blue color) performed by the tool tip.

Figure 7, Figure 8, Figure 9 shows the three different virtual task shapes generated in an augmented reality 3D environment. The green dotted line represent the virtual task generated in the augmented reality 3D environment and the blue line represent the path followed by the end-effector's tool tip autonomously. This gives the sensation of a real surgical operation inside a patient's organ. This path following task can be visualized directly on the surgeon's console (master PC) with the help of an HD endoscopic camera.

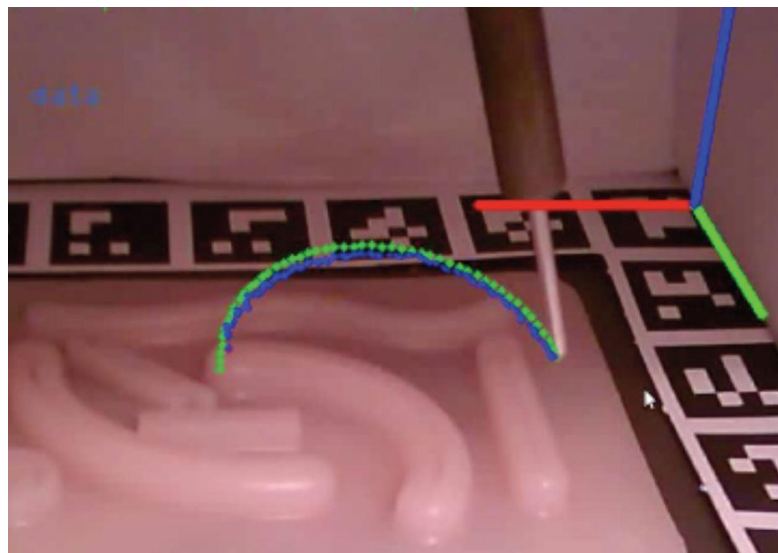


Figure 7. Task 1 representing a half-ellipsoidal wave

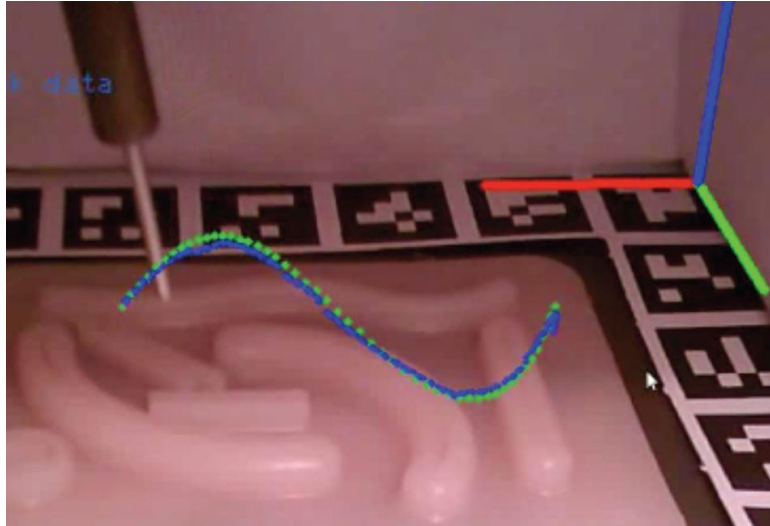


Figure 8. Task 2 representing a sine wave

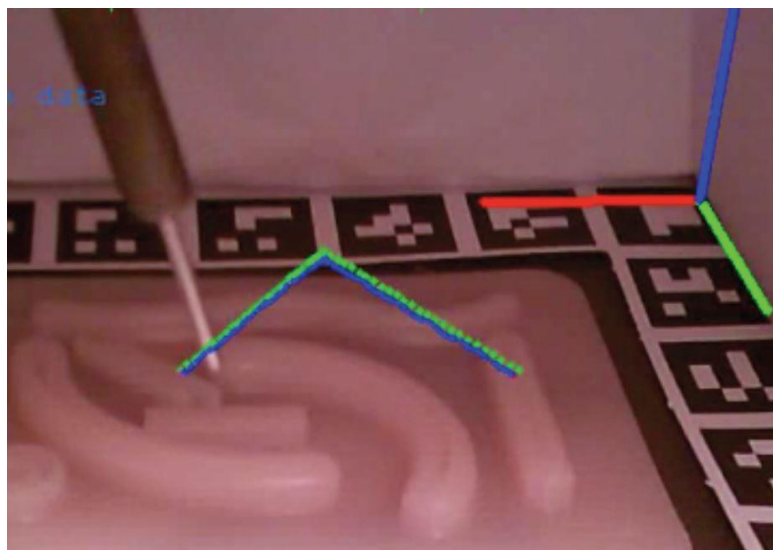


Figure 9. Task 3 representing a triangular wave

Cartesian Compliance Controller (CCC)

The dynamic model of a 7-DoF serial manipulator in the Lagrangian formulation can be expressed as:

$$M(q)\ddot{q} + C(q, \dot{q})\dot{q} + g(q) = \tau_C - \tau_{EXT} \quad (23)$$

where $q \in \mathbb{R}^7$ is the vector of joint coordinates, $M(q) \in \mathbb{R}^{7 \times 7}$ is the inertia matrix, $C(q, \dot{q}) \in \mathbb{R}^{7 \times 7}$ is a matrix representing the Coriolis and centrifugal terms, and $g(q) \in \mathbb{R}^7$ is the vector of gravitational torques. Torque vectors $\tau_C \in \mathbb{R}^7$ and $\tau_{EXT} \in \mathbb{R}^7$ represent the control torque and the external torque vectors respectively. The following inverse dynamics control solution can be introduced as:

$$\tau_C = \tau_d + \tau_{dynamics} + \hat{\tau}_{EXT} \quad (24)$$

$$\tau_{dynamics} = \hat{M}(q)\ddot{q} + \hat{C}(q, \dot{q})\dot{q} + \hat{g}(q) \quad (25)$$

where $\tau_{dynamics}$ is the estimated dynamics provided by the KUKA Fast Research Interface (FRI) [21]. $\hat{M}(q) \in \mathbb{R}^{7 \times 7}$ is the estimated inertia matrix, $\hat{C}(q, \dot{q}) \in \mathbb{R}^{7 \times 7}$ and $\hat{g}(q) \in \mathbb{R}^7$ are the estimated compensation terms, $\hat{\tau}_{EXT}$ is the filtered torque computed from the external torque sensors, and τ_d is an additive control term introduced to achieve control objective. The main task for the MIS robot is tracking the desired Cartesian trajectory generated by the surgeon [23], [24], while guaranteeing safety by way of a Cartesian impedance controller. First of all, to guarantee the required smoothness and avoid the trajectory generated by the surgeon exceeds the robot acceleration and velocity constraints, an interpolation function is introduced. In particular, the surgeon trajectory is interpolated using a 5th order polynomial in Cartesian space [25], adapting the trajectory duration in such a way that the maximum Cartesian acceleration and velocity constraints are satisfied. Then, a cartesian space compliance control term, $\tau_T \in \mathbb{R}^7$, can be introduced as:

$$\tau_T = J_T^T(q) \left(-K_X(X - X_d) - D_X(\dot{X} - \dot{X}_d) \right) \quad (26)$$

where $D_X, K_X \in \mathbb{R}^{3 \times 3}$ are the diagonal damping and stiffness matrices, respectively. $X_d, \dot{X}_d \in \mathbb{R}^3$ are the desired position and velocity trajectories, respectively, and $J_T(q) \in \mathbb{R}^{3 \times 7}$ is the Jacobian matrix from the base frame to the end-effector. The magnitude of the Cartesian position error can be written as in [26]:

$$\|E_X\| = \|X_d - X\| \quad (27)$$

For simplicity, it is assumed that the surgical robot is far away from singularities, and the pseudo-inverse of J_T exists. This cartesian compliance controller developed is almost the same as in [6]. The overall control scheme is shown in Figure 10 where the CCC controller and the AFC controller can be seen with their inputs and outputs.

Adaptive Fuzzy Controller (AFC)

The adaptive fuzzy controller is implemented into the robot exactly as in [6] and the control equations are as follows:

$$\tau_F = -J^T \Theta \xi(X, \dot{X}, \psi, \dot{\psi}) \quad (28)$$

where

$J^T \in \mathbb{R}^{6 \times 7}$ is the jacobian matrix;

$\Theta = [\theta_1, \theta_2, \dots, \theta_6]^T \in \mathbb{R}^{6 \times 7}$ is a weight parameter matrix;

$\theta_i \in \mathbb{R}^{7 \times 1}, i = 1, 2, \dots, 6$

$\xi(X, \dot{X}, \psi, \dot{\psi}) = [\xi_1, \xi_2, \dots, \xi_7] \in \mathbb{R}^{7 \times 1}$ is the adaptive basis functions as defined in [6].

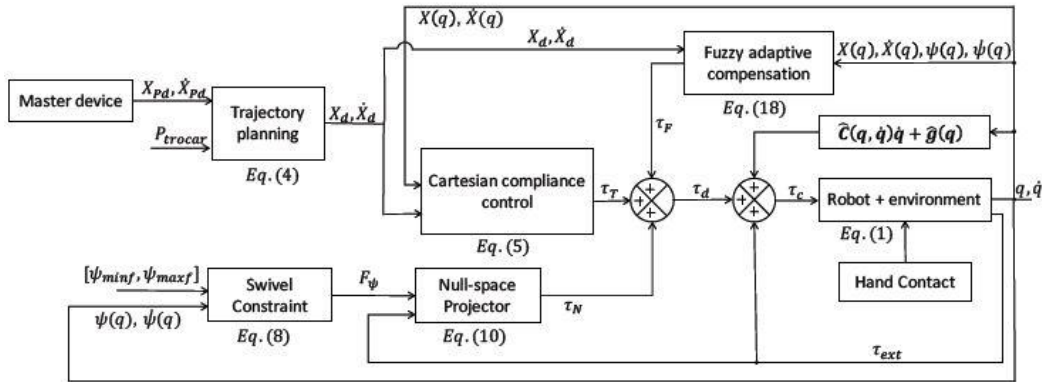


Figure 10. Block diagram of Overall System with two controllers (CCC & AFC)

Chapter 3

Statistical Analysis of Experimental Results

Experimental Validation

The experimental set-up is done as described in the Chapter. The robot is programmed to autonomously follow a path generated by the “vision computer”. The end-effector’s tool tip follows the task path generated in the cartesian space (i.e. 3 different task shapes: a half-ellipsoidal wave, a sine wave and a triangular wave). In order to make a statistical analysis, we would like to have sufficient data to be processed. Taking this into consideration, six different experimental trials (test1, test2, ..., test6 as shown in Table 6) were executed with the two controllers (CCC and AFC) alternatively for three different tasks as shown in Figure 7, Figure 8 and Figure 9 (named as T1, T2 and T3). The aim of this chapter is to acquire the data from the experimental trials and group them for further statistical analysis to compare the performance among two controllers (CCC and AFC) with respect to the parameters: Cartesian positional error and RCM constraint error. The experimental grouping of data can be seen in Table 6.

Parameter	Tests	Task	Controller
Cartesian Positional Error	Test1	T1	CCC
	Test2	T1	AFC
	Test 3	T2	CCC
	Test 4	T2	AFC
	Test 5	T3	CCC
	Test 6	T3	AFC
RCM constraint Error	Test1	T1	CCC
	Test2	T1	AFC
	Test 3	T2	CCC
	Test 4	T2	AFC
	Test 5	T3	CCC
	Test 6	T3	AFC

Table 6. Experimental grouping of Data

Data Grouping

Once the experimental trials are executed, the data obtained can be visualized as shown in Figure 11 (desired cartesian position along x and y axis for CCC in one test), Figure 13 (actual cartesian position along x and y axis for CCC). The z-axis is not shown here, as it does not have much variations and only the x-axis is useful for finding the task range for further processing and grouping. Figure 12, Figure 14 depicts the enlarged image of x-axis with series of different tasks executed using the CCC controller.

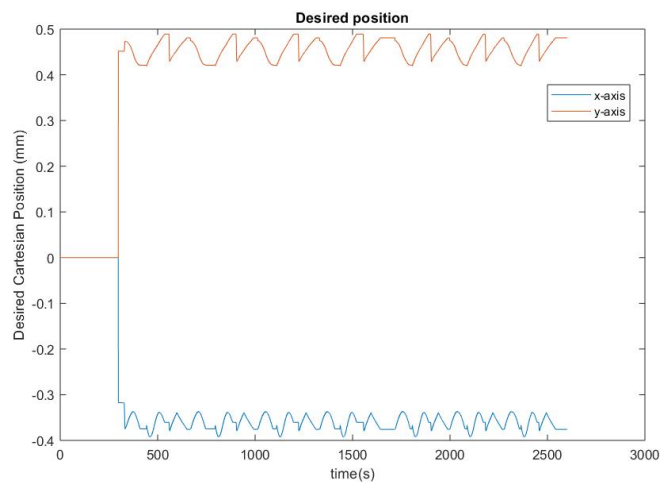


Figure 11. Desired Cartesian position by following three different task shapes for CCC

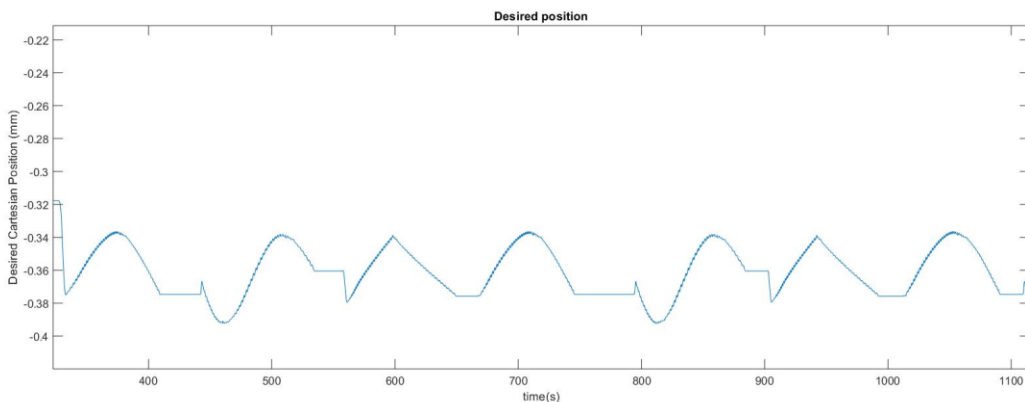


Figure 12. Enlarged image of x-axis with series of three different tasks for CCC

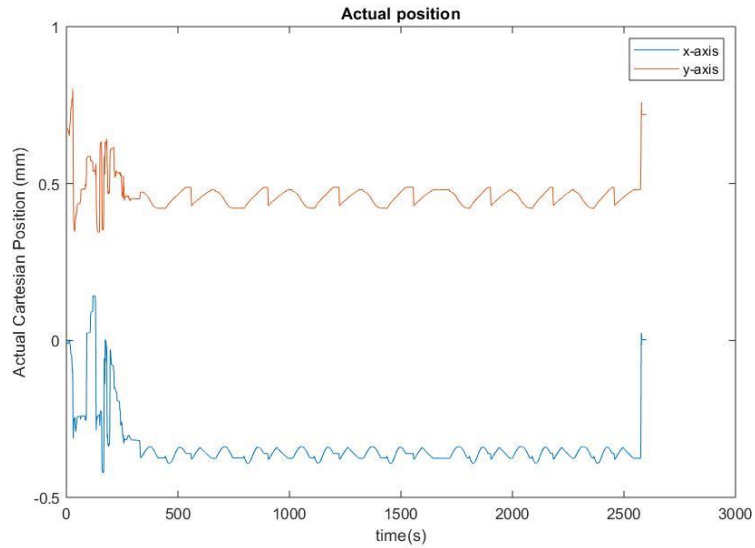


Figure 13. Actual Cartesian position by following three different task shapes for CCC

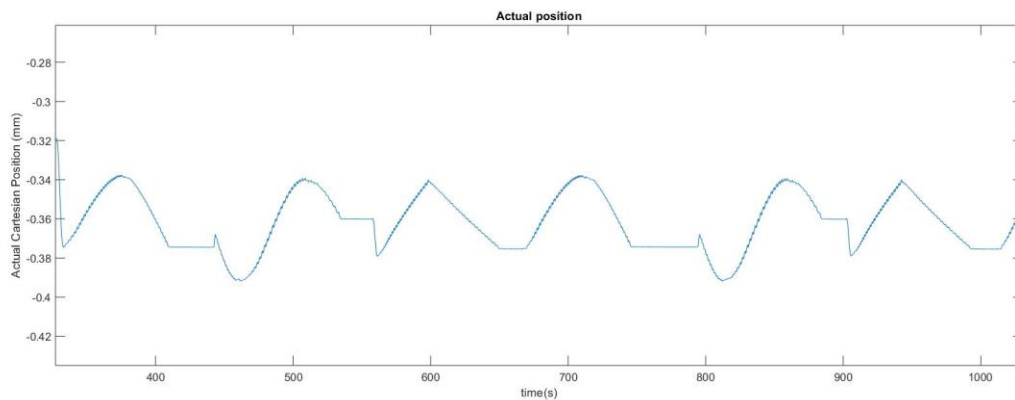


Figure 14. Enlarged image of x-axis with series of three different tasks for CCC

The grouping of the data after the experimental trials are executed exactly as per the following steps:

- Since there are sudden jumps during the experiment either at the beginning or ending of each task, the complete data cannot be taken into account. The data is taken precisely for each task (by cutting exactly the task shape) with respect to time for each controller (CCC and AFC). This process is repeated also for the data of actual Cartesian position.

Using the data obtained from the previous step for desired and actual task paths, the Cartesian positional error is calculated as discussed in eq. (29).

- This returns a vector of data that can be grouped and processed.
- Finally, the collected data can be grouped as per the controllers (test1, test3 and test5 are grouped together for CCC, whereas test2, test4 and test6 are grouped together for AFC) and executed with the data analysis procedures for each cases.

Similarity of two curves using Fréchet Distance

Another technique to calculate the distance among the two curves (for e.g. in our case, the desired cartesian position and the actual cartesian position for each task) is called “**Fréchet distance**” [27]. It returns the distance as a measure of similarity between two curves, say P and Q. It is defined as the minimum cord-length sufficient to join a point travelling forward along P and one travelling forward along Q, although the rate of travel of either point may not necessarily be uniform. Fréchet distance is available as a functional script in MATLAB [28]. If Fréchet distance as in [28] is applied to our scenario, let’s say, among the task 1’s desired and actual curves, it returns only a scalar distance value. This cannot be considered for further data processing because there are only six scalar values (one for each test) which are not sufficient enough to make neither a box-plot nor to analyze using any statistical tools. For this reason, Fréchet distance cannot be applied to our scenario.

Statistical Analysis-Case1

The main aim of this case is to check the performance of each controller with respect to the **Cartesian positional error**.

Normality Check

After completing the process of grouping, the data collected for cartesian positional error (test1, test3 and test5 together for CCC and test2, test4 and test6 together for AFC) were checked for normality distribution using the Kolmogorov-Smirnov test and Lilliefors’s test. Lilliefors’s test and Kolmogorov- Smirnov test are available as MATLAB functions which returns binary values as a result of normality check (0 for normal distribution and 1 for non- normal distribution). The grouped

data failed for its normality distribution in both of the test. The distributions can also be viewed as histograms as shown in Figure 15, thereby violating the important assumption of ANOVA. The non-normally distributed data is depicted in Figure 15. Due to its non-normality distribution, the comparison of the groups cannot be executed with ANOVA unless the data are normalized. The probability of a type I error is more if ANOVA is used. Hence, Kruskal-Wallis is the best bet in this scenario.

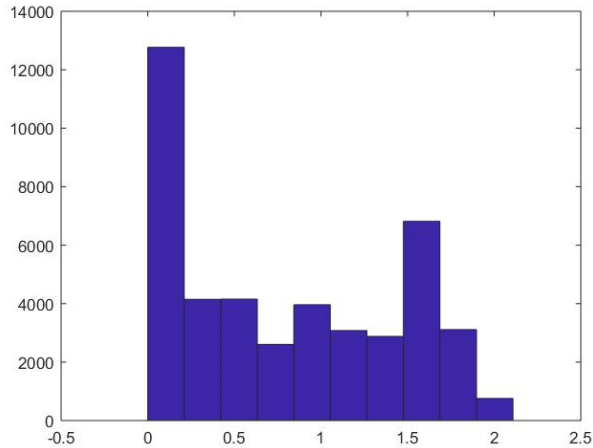


Figure 15. Non-normally distributed data for Cartesian positional error

Kruskal-Wallis Test for Cartesian Positional Error Analysis

The Kruskal-Wallis test was performed for each task group against the two controllers and the following box-plot shows the significant differences among the groups. (**Null hypothesis:** The means of all the tasks in CCC are same).

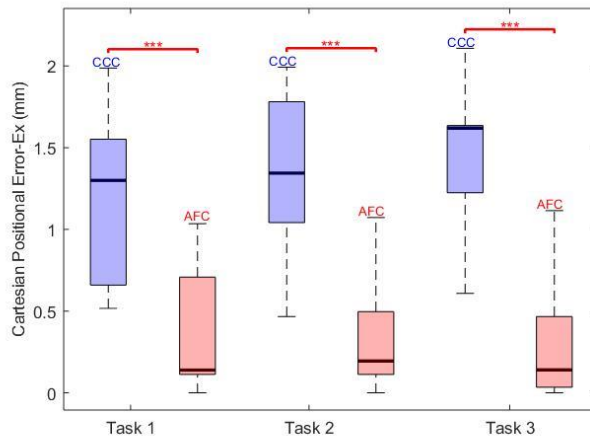


Figure 16. Box-plot for three different tasks with two controllers

It can be seen from Figure 16 that the test1, test3 and test5 are shown in blue color to represent the CCC whereas test2, test4 and test6 are shown in light orange color to represent the AFC. Each box represents the tests in the ascending order of 1 to 6 (left to right in Figure 16). For each task, both the controllers are compared (test1 and test2; test3 and test4; test5 and test6) and the significant differences are obtained.

The following tables (Table 7, Table 8 and Table 9) represent the Kruskal-Wallis one-way ANOVA table that shows the significant differences among groups.

Kruskal-Wallis one-way ANOVA table					
Source	SS	df	MS	Chi-sq	Prob>Chi-sq
Groups	1.91875e+10	1	1.91875e + 10	3519.35	0
Error	2.49028e+10	8086	3.079794e + 06		
Total	4.40902e+10	8087			

Table 7. Task1 significant difference among controllers

Kruskal-Wallis one-way ANOVA table					
Source	SS	df	MS	Chi-sq	Prob>Chi-sq
Groups	9.06896e+10	1	9.06896e+10	6853.22	0
Error	7.6048e+10	12599	6.03603e+06		
Total	1.66738e+11	12600			

Table 8.Task2 significant difference among controllers

Kruskal-Wallis one-way ANOVA table					
Source	SS	df	MS	Chi-sq	Prob>Chi-sq
Groups	7.36201e+11	1	7.36201e+11	15873.29	0
Error	3.579e+11	23589	1.51723e+07		
Total	1.0941e+12	23590			

Table 9.Task3 significant difference among controllers

It is clearly evident that each tasks are significantly different from each other among the controllers compared (CCC and AFC). The p-values (last column of the Kruskal-Wallis ANOVA table) seems to be less than 0.001 ($p < 0.001$) with a very high significant difference as described in Table 3.

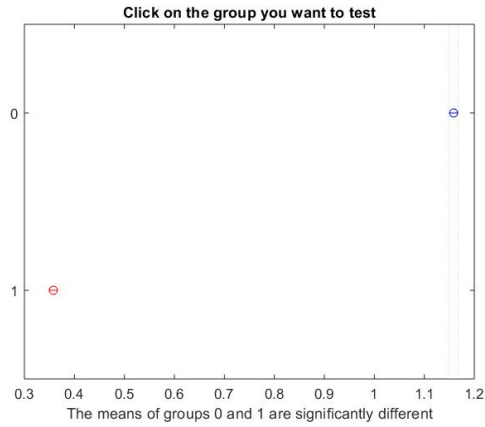


Figure 17. Significant Difference between CCC and AFC for task 1

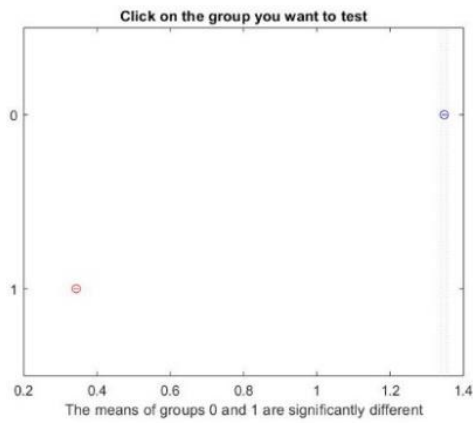


Figure 18. Significant Difference between CCC and AFC for task 2

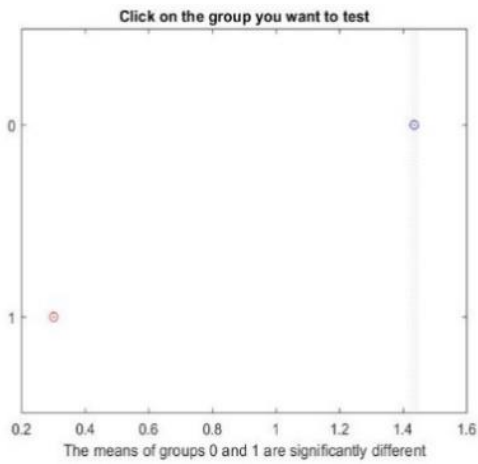


Figure 19. Significant Difference between CCC and AFC for task 3

The above figures Figure 17, Figure 18 and Figure 19 display the result of the Tukey's post-hoc test which confirms that there is a significant level of differences between both the controllers for each task ($p < 0.001$). Post-hoc tests are required only in cases of more than 3 groups involved in the study to find which two group differed significantly. For example, if there are at least 5 controller groups that needs to be compared, ANOVA and Kruskal-Wallis tells if there are significant differences among the groups compared, but the post-hoc test tells us which groups exactly have a significant difference with respect to other groups. In our scenario, there are only two groups for comparison and hence the post-hoc test is not used throughout.

Comparison among tasks in CCC controller

Proceeding further to analyze the effect of the three tasks for the same controller, the same procedure was adopted and the corresponding box-plots and Kruskal-Wallis ANOVA table can be depicted as follows:

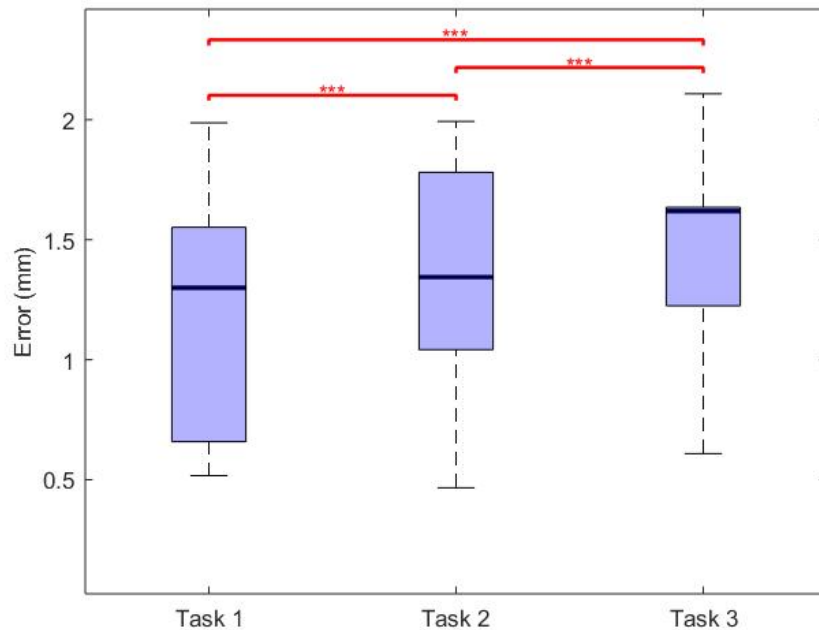


Figure 20.Box-plot of three different tasks for CCC controller

Kruskal-Wallis one-way ANOVA table					
Source	SS	df	MS	Chi-sq	Prob>Chi-sq
Groups	2.41282e+09	1	2.41282e+09	336.17	4.3485e-75
Error	6.41854e+10	9278	6.91802e+06		
Total	6.65982e+10	9279			

Table 10.Task1 and 2 comparison using CCC controller

Kruskal-Wallis one-way ANOVA table					
Source	SS	df	MS	Chi-sq	Prob>Chi-sq
Groups	5.38134e+08	1	5.38134e+08	26.35	2.84696e-07
Error	3.19126e+11	15652	2.03888e+07		
Total	3.19664e+11	15653			

Table 11.Task2 and 3 comparison using CCC controller

Kruskal-Wallis one-way ANOVA table					
Source	SS	df	MS	Chi-sq	Prob>Chi-sq
Groups	3.43149e+10	1	3.43149e+10	1519.41	0
Error	3.37448e+11	16460	2.05011e+07		
Total	3.71762e+11	16461			

Table 12.Task1 and 3 comparison using CCC controller

The box-plot shows the significant differences among the three tasks (test1, test3 and test5) for the same CCC controller. The $p\text{-value} < 0.001$ for all the three tasks when compared with each other (Table 10, Table 11 and Table 12). This fact clearly proves that the CCC controller was highly influenced by the three virtual tasks.

Comparison among tasks in AFC controller

The data analysis procedure is repeated for the data obtained for the AFC controller for all the three tasks (test2, test4 and test6) and the corresponding box-plots and the Kruskal-Wallis table are reported below.

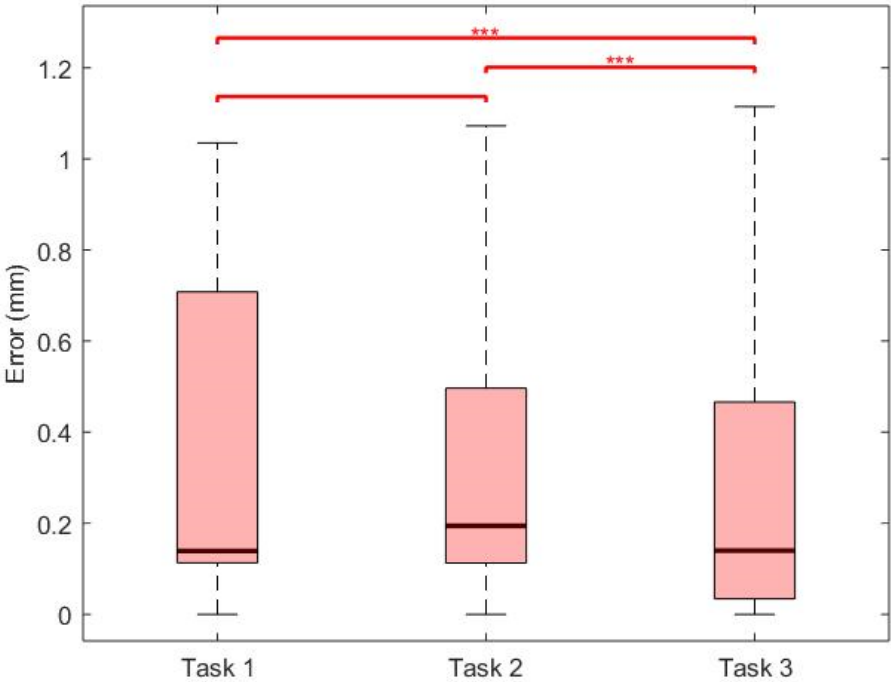


Figure 21.Box-plot of three different tasks for AFC controller

Kruskal-Wallis one-way ANOVA table					
Source	SS	df	MS	Chi-sq	Prob>Chi-sq
Groups	991346.4	1	991346.4	0.09	0.7624
Error	123753590249.1	11407	10848916.5		
Total	123754581595.5	11408			

Table 13.Task1 and 2 comparison using AFC controller

Kruskal-Wallis one-way ANOVA table					
Source	SS	df	MS	Chi-sq	Prob>Chi-sq
Groups	6.12752e+09	1	6.12752e+09	174.31	8.45944e-40
Error	7.15799e+11	20536	3.48558e+07		
Total	7.21927e+11	20537			

Table 14.Task2 and 3 comparison using AFC controller

Kruskal-Wallis one-way ANOVA table					
Source	SS	df	MS	Chi-sq	Prob>Chi-sq
Groups	7.49552e+09	1	7.49552e+09	388.42	1.83158e-86
Error	2.86138e+11	15215	1.88063e+07		
Total	2.93633e+11	15216			

Table 15.Task1 and 3 comparison using AFC controller

The tasks with AFC controller are shown in the Figure 21 where there are no significant differences among the task 1 and 2. This could be further attested by the p-value obtained by the Kruskal-Wallis table in Table 13. The other two task groups show significant differences among each other which is also attested by the Kruskal-Wallis one-way ANOVA table in Table 14 and Table 15.

In case of ANOVA was used to check these data directly, the chances of obtaining the type I error is clear from Table 16 .Although the Kruskal-Wallis test reported that the task group 1 and 2 did not have any significant difference, the ANOVA for the non- normally distributed data clearly shows a significant difference which is a false positive.

One-way ANOVA table					
Source	SS	df	MS	F	p
Groups	0.47	1	0.47312	4.07	0.0438
Error	1327.23	11407	0.11635		
Total	1327.71	11408			

Table 16.Task1 and 2 comparison using AFC controller-ANOVA (False Positive)

Statistical Analysis-Case2

The main aim of this case is to check the performance of each controller (CCC & AFC) with respect to the **Remote Center of Motion (RCM) constraint error**.

Data Grouping

Unlike the Cartesian positional error, the RCM error is computed online and the acquired data is the result of RCM constraint error and it is shown in Figure 22. Figure 23 shows the enlarged image with all the tasks, but does not represent the

exact task shape. Hence, one should be careful in separating the RCM error data for each task. The precise data has to be taken into consideration and so the RCM error with respect to time for each task is separated (by cutting each tasks accurately with respect to time). This can also be done by selecting the range for each task shapes that was obtained from the desired Cartesian position which had all the tasks with respect to time. This yields the exact RCM error for each task using different controllers' data.

Finally, the collected data can be grouped as per the controllers (test1, test3 and test5 are grouped together for CCC, whereas test2, test4 and test6 are grouped together for AFC) as shown in Table 6 and executed with the data analysis procedure.

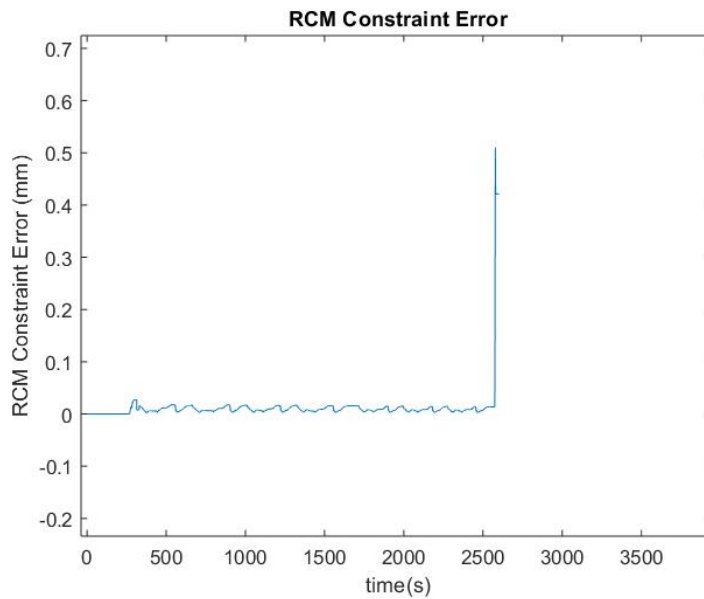


Figure 22. RCM Error by following three different task shapes for CCC

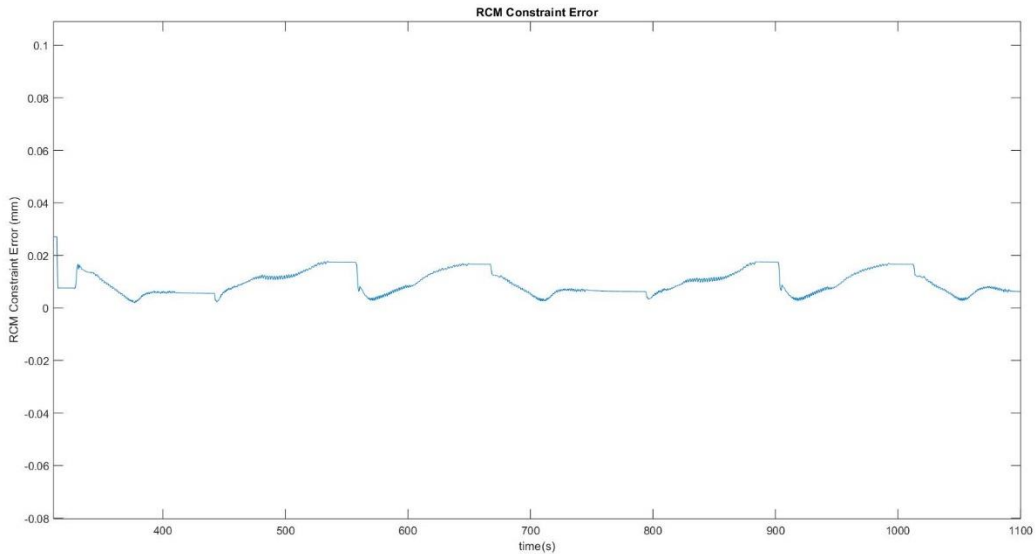


Figure 23. Enlarged image with series of three different tasks for CCC

Normality Check

The data collected for RCM error are checked for normality distribution using the Kolmogorov- Smirnov (KS) test and Lilliefors's (LS) test. The data failed for its normality distribution in both the tests, violating the primary assumption of ANOVA. The non-normally data is depicted in Figure 24 as a histogram. Due to its non- normality distribution, the comparison of the groups cannot be executed with ANOVA unless the data are normalized. The probability of a type I error is more if ANOVA is used. Hence, Kruskal-Wallis is the best bet in this situation.

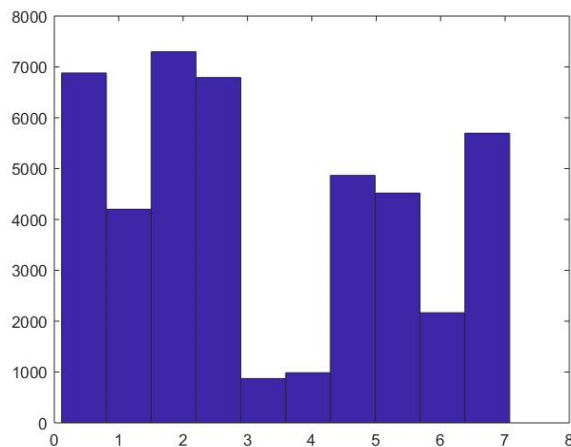


Figure 24. Non-normal distribution of data for RCM error

Kruskal-Wallis Test for Remote Center of Motion (RCM) Error Analysis

The Kruskal-Wallis test was performed for each task group (test1 and test2; test3 and test4; test5 and test6) against the two controllers and the following box-plot shows the significant differences among the groups. (**Null hypothesis:** The means of all the tasks in controller CCC are same).

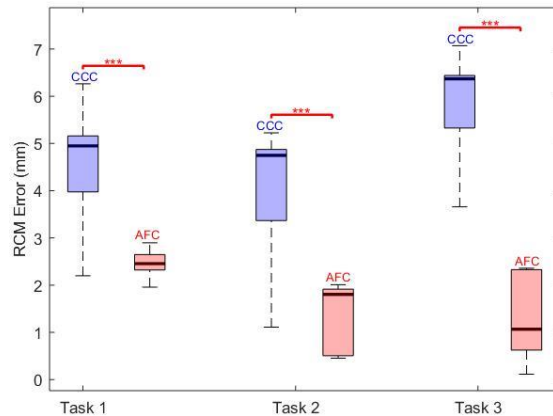


Figure 25.Box-plot of three different tasks for RCM error

It can be seen from Figure 25 that the test1, test3 and test5 are shown in blue color to represent the CCC whereas test2, test4 and test6 are shown in light orange color to represent the AFC. Each box represents the tests in the ascending order of 1 to 6 (from left to right in Figure 25). For each task, both the controllers are compared (test1 and test2; test3 and test4; test5 and test6) and the significant differences are obtained.

Kruskal-Wallis one-way ANOVA table					
Source	SS	df	MS	Chi-sq	Prob>Chi-sq
Groups	1.98624e+10	1	1.98624e+10	3643.15	0
Error	2.42278e+10	8086	2.99627e+06		
Total	4.40902e+10	8087			

Table 17.Task1 significant difference among controllers

Kruskal-Wallis one-way ANOVA table					
Source	SS	df	MS	Chi-sq	Prob>Chi-sq
Groups	7.17706e+10	1	7.17706e+10	5423.54	0
Error	9.49671e+10	12599	7.53767e+06		
Total	1.66738e+11	12600			

Table 18.Task2 significant difference among controllers

Kruskal-Wallis one-way ANOVA table					
Source	SS	df	MS	Chi-sq	Prob>Chi-sq
Groups	8.19736e+11	1	8.19736e+11	17674.4	0
Error	2.74365e+11	23589	1.1631e+07		
Total	1.0941e+12	23590			

Table 19.Task3 significant difference among controllers

It is clearly evident that each tasks are significantly different from each other among the controllers compared. The p-values are less than 0.001 ($p < 0.001$) with a very high significant difference.

Comparison among tasks in CCC controller

Proceeding further to analyze the effect of the three tasks (test1, test3 and test5) for the same controller (CCC), the same procedure is adopted and the corresponding box-plots and Kruskal-Wallis ANOVA table can be depicted as follows:

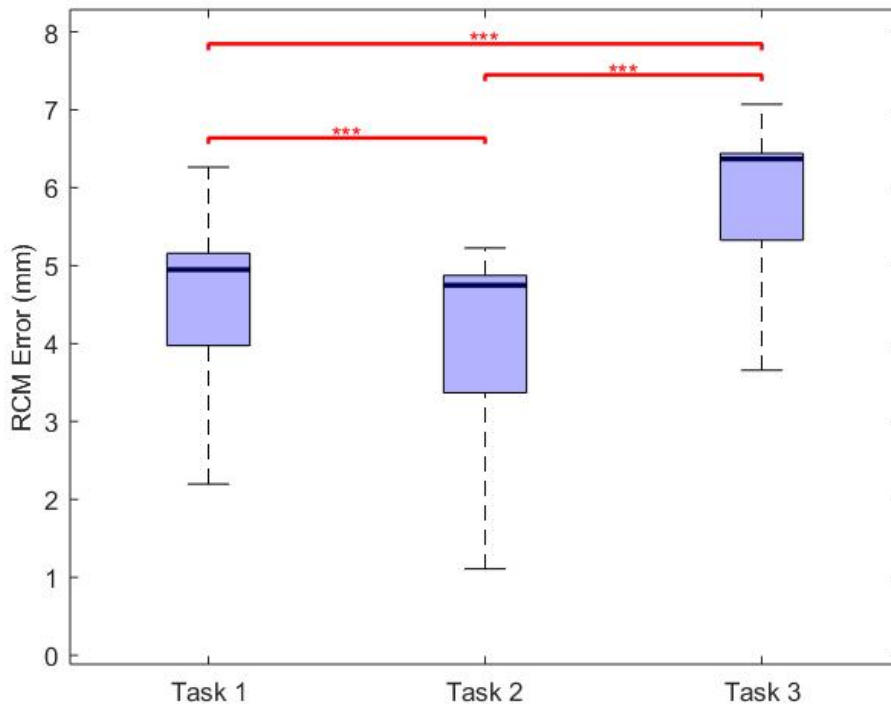


Figure 26.Box-plot of three different tasks for CCC controller

Kruskal-Wallis one-way ANOVA table					
Source	SS	df	MS	Chi-sq	Prob>Chi-sq
Groups	5.45984e+09	1	5.45984e+09	760.71	1.8837e-167
Error	6.11384e+10	9278	6.58961e+06		
Total	6.65982e+10	9279			

Table 20.Task1 and 2 comparison using CCC controller

Kruskal-Wallis one-way ANOVA table					
Source	SS	df	MS	Chi-sq	Prob>Chi-sq
Groups	1.2006e+11	1	1.2006e+11	5878.99	0
Error	1.99604e+11	15652	1.27526e+07		
Total	3.19664e+11	15653			

Table 21.Task2 and 3 comparison using CCC controller

Kruskal-Wallis one-way ANOVA table					
Source	SS	df	MS	Chi-sq	Prob>Chi-sq
Groups	1.09977e+11	1	1.09977e+11	4869.62	0
Error	2.61785e+11	16460	1.59043e+07		
Total	3.71762e+11	16461			

Table 22.Task1 and 3 comparison using CCC controller

The box-plot shows the significant differences among the three tasks for the same CCC controller. The p -value < 0.001 for all the three tasks when compared with each other (Table 20, Table 21 and Table 22). This fact clearly proves that the CCC controller was highly influenced by the three tasks created to analyze the RCM error.

Comparison among tasks in AFC controller

The data analysis procedure is repeated for the data obtained for the AFC controller group (test2, test4 and test6 - boxes from left to right in Figure 27) for all the three tasks to analyze the RCM error and the corresponding box-plots and the Kruskal-Wallis table are reported below.

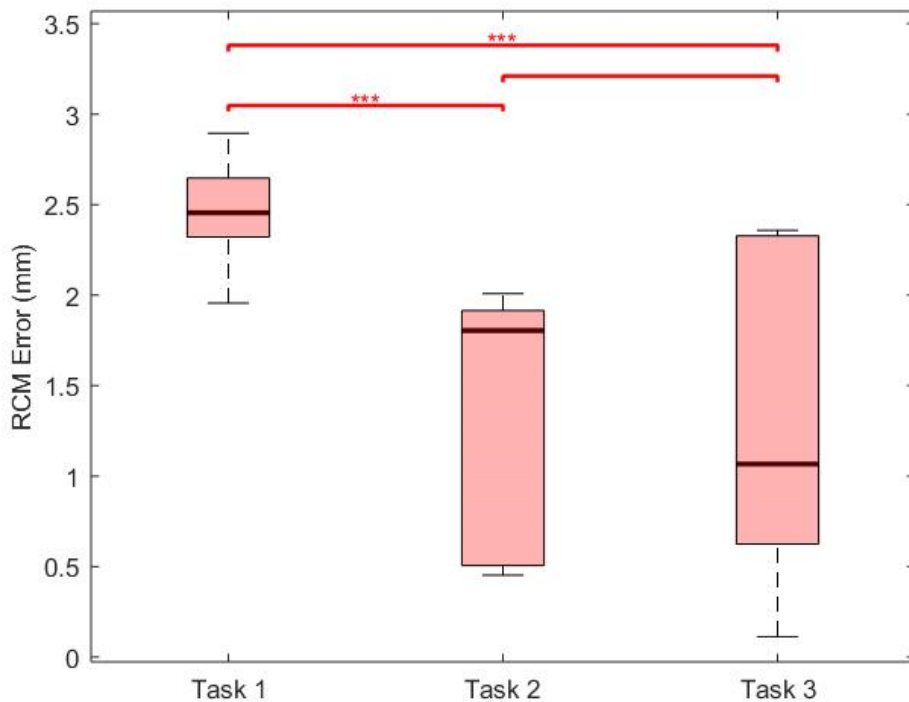


Figure 27.Box-plot of three different tasks for AFC controller

Kruskal-Wallis one-way ANOVA table					
Source	SS	df	MS	Chi-sq	Prob>Chi-sq
Groups	7.25709e+10	1	7.25709e+10	6689.76	0
Error	5.11837e+10	11407	4.48704e+06		
Total	1.23755e+11	11408			

Table 23.Task1 and 2 comparison using AFC controller

Kruskal-Wallis one-way ANOVA table					
Source	SS	df	MS	Chi-sq	Prob>Chi-sq
Groups	3.45814e+06	1	3.45814e+06	0.1	0.7538
Error	7.21923e+11	20536	3.5154e+07		
Total	7.21927e+11	20537			

Table 24.Task2 and 3 comparison using AFC controller

Kruskal-Wallis one-way ANOVA table					
Source	SS	df	MS	Chi-sq	Prob>Chi-sq
Groups	1.00118e+11	1	1.00118e+11	5188.08	0
Error	1.93516e+11	15215	1.27187e+07		
Total	2.93633e+11	15216			

Table 25.Task1 and 3 comparison using AFC controller

The tasks with AFC controller are shown in the Figure 27 where there are no significant differences among the task 2 and 3. This could be further attested by the p-value obtained by the Kruskal-Wallis table in Table 24. The other two task groups show significant differences among each other which is also attested by the Kruskal-Wallis one-way ANOVA table in Table 23 and Table 25.

Chapter 4

Discussion and Conclusion

From the above experimental comparisons and data analysis among the two controllers with respect to Cartesian positional error and RCM constraint error, the following discussion and conclusion can be drawn as follows:

- The Cartesian Compliance Controller (CCC)'s data, the box-plots in Figure 16, Figure 20 depicts the significant differences among the three tasks with respect to the Cartesian positional error. The Kruskal-Wallis one-way ANOVA tables (Table 10, Table 11 and Table 12) also confirms the significant difference with p-value <0.001 . With these observations, we can conclude that the three tasks (T1, T2 and T3) influences the CCC controller to a larger extent with the data obtained with respect to the Cartesian positional error.
- At the same time, the Adaptive Fuzzy controller (AFC) for the data obtained with respect to the Cartesian positional error shows that the tasks 1 and 2 had no significant differences. This could be caused due to the fact that the task 1 (half-ellipsoid) and task 2 (sine-wave) were almost similar in the first half part of their shape similarity. The other task groups 2 and 3; task 1 and 3 showed significant differences.
- The Cartesian Compliance Controller (CCC)'s data for the RCM constraint error depicts the significant differences among the three tasks as shown in Figure 25, Figure 26. The Kruskal-Wallis one-way ANOVA tables (Table 20, Table 21 and Table 22) also confirms the significant difference with p-value <0.001 . These observations confirms that the three tasks (T1, T2 and T3) influences the CCC controller to a larger extent with the data obtained with respect to the RCM constraint error.
- The Adaptive Fuzzy controller (AFC) for the data obtained with respect to the RCM constraint error shows that the tasks 2 and 3 had no significant differences. This could be caused due to the fact that the task 2 (sine-wave) and task 3 (triangular-wave) accomplished the virtual task by respecting their RCM constraint. The other task groups 1 and 2; task 1 and 3 showed significant differences.

From all the analysis of data using the one-way ANOVA of Kruskal-Wallis, we can conclude that the **significant differences among the task groups were reduced using the AFC controller for both RCM constraint error as well as Cartesian positional error**. From the box-plots, the Adaptive Fuzzy Controller (AFC) had reduced errors compared with the other controller. Thus, **Adaptive Fuzzy Controller (AFC) performed better than the Cartesian Compliance Controller (CCC)** in terms of RCM constraint error and Cartesian positional error.

References

- [1] A. R. Lanfranco, A. E. Castellanos, J. P. Desai and W. C. Meyers, "Robotic surgery: a current perspective," *Annals of surgery*, Vols. 239,, no. 1, p. 14, 2004.
- [2] N. Aghakhani, M. Geravand, N. Shahriari, M. Vendittelli and G. Oriolo, "Task control with remote center of motion constraint for minimally," *IEEE International Conference on Robotics and Automation (ICRA)*, p. 5807–5812, 2013.
- [3] G. Ferrigno and E. D. Momi, "Robotic and artificial intelligence for keyhole neurosurgery: the ROBOCAST project, a multi-modal autonomous path planner," *Proceedings of the Institution of Mechanical Engineers, Part H: Journal of Engineering in Medicine*, vol. 224, no. 5, p. 715–727, 2010.
- [4] H. Azimian, R. V. Patel and M. D. Naish, "On constrained manipulation in robotics-assisted minimally invasive surgery," *Biomedical Robotics and Biomechatronics (BioRob) , 2010 3rd IEEE RAS and EMBS International Conference*, p. 650–655, 2010.
- [5] H. Sadeghian, F. Zokaei and S. H. Jazi, "Constrained kinematic control in minimally invasive robotic surgery subject to remote center of motion constraint," *Journal of Intelligent & Robotic Systems*, p. 1–13, 2018.
- [6] H. Su, J. Sandoval, M. Makhdoomi, G. Ferrigno and E. D. Momi, "Safety-enhanced Human-Robot Interaction Control of Redundant Robot for Teleoperated Minimally Invasive Surgery," *IEEE International Conference on Robotics and Automation (ICRA)*, 2018.
- [7] R. A. Fisher, "The Correlation Between Relatives on the Supposition of Mendelian Inheritance," *Philosophical Transactions of the Royal Society of Edinburgh*, vol. 52, p. 399–433, 1918.
- [8] Neyman, "[On the Application of Probability Theory to Agricultural Experiments. Essay on Principles. Section 9.] Comment: Neyman (1923) and

- Causal Inference in Experiments and Observational Studies," *Statistical Science*, vol. 5, no. 4, pp. 472-480, 1990.
- [9] O. Kempthorne, "The design and analysis of experiments," *Oxford, England: Wiley*, 1952.
- [10] E. J. G. Pitman, "Significance Tests Which May be Applied to Samples From any Populations," *Supplement to the Journal of the Royal Statistical Society*, vol. 4, no. 1, pp. 119-130, 1937.
- [11] Kruskal and Wallis, "Use of ranks in one-criterion variance analysis," *Journal of the American Statistical Association*, p. 583–621, 1952.
- [12] G. W. Corder and D. I. Foreman, "Nonparametric Statistics for Non-Statisticians," *Hoboken: John Wiley & Sons*, p. 99–105, 2009.
- [13] Siegel and Castellan, "Nonparametric Statistics for the Behavioral Sciences (Second ed.)," *New York: McGraw–Hill*, 1988.
- [14] O. J. Dunn, "Multiple comparisons using rank sums," *Technometrics*, vol. 6, no. 3, p. 241–252, 1964.
- [15] W. J. Conover and R. L. Iman, "On multiple-comparisons procedures," Los Alamos Scientific Laboratory, 1979.
- [16] Scheffé and Henry, "The Analysis of Variance," *New York: Wiley*, 1959.
- [17] L. Statistics, "Kruskal-Wallis H Test using SPSS Statistics," [Online]. Available: <https://statistics.laerd.com/spss-tutorials/kruskal-wallis-h-test-using-spss-statistics.php>.
- [18] F. Wilcoxon, "Individual Comparisons by Ranking Methods," *Biometrics Bulletin*, vol. 1, no. 6, pp. 80-83, 1945.
- [19] J. D. Spurrier, "On the null distribution of the Kruskal–Wallis statistic," *Journal of Nonparametric Statistics*, vol. 15, no. 6, p. 685–691, 2003.
- [20] "Values of the Chi-squared distribution," [Online]. Available: <https://www.medcalc.org/manual/chi-square-table.php>.

- [21] G. Schreiber, A. Stemmer and R. Bischoff, "The fast research interface for the kuka lightweight robot," *IEEE Workshop on Innovative Robot Control Architectures for Demanding (Research) Applications How to Modify and Enhance Commercial Controllers (ICRA 2010)*, p. 15–21, 2010.
- [22] S. Garrido Jurado, R. Munoz Salinas, F. J. Madrid Cuevas and M. Marin Jimenez, "Automatic generation and detection of highly reliable fiducial markers under occlusion," *Pattern Recognition*, vol. 47, no. 6, p. 2280–2292, 2014.
- [23] H. Kang and J. T. Wen et al., "Autonomous suturing using minimally invasive surgical robots," *Proceedings of the 2000 IEEE International Conference on Control Applications. IEEE*, p. 742–747, 2000.
- [24] A. Krupa, J. Gangloff, C. Doignon, M. F. D. Mathelin, G. Morel, J. Leroy, L. Soler and J. Marescaux, "Autonomous 3-d positioning of surgical instruments in robotized laparoscopic surgery using visual servoing," *IEEE transactions on robotics and automation*, vol. 19, no. 5, p. 842–853, 2003.
- [25] J. Sandoval, H. Su, P. Vieyres, G. Poisson, G. Ferrigno and E. D. Momi, "Collaborative framework for robot-assisted minimally invasive surgery using a 7-dof anthropomorphic robot," *Robotics and Autonomous Systems*, vol. 106, p. 95–106, 2018.
- [26] H. Su, S. Li, J. Manivannan, L. Bascetta, G. Ferrigno and E. D. Momi, "Manipulability Optimization Control of a Serial Redundant Robot for Robot-assisted Minimally Invasive Surgery," in *International Conference of Robotics and Automation*, Montreal, 2019.
- [27] A. J. Ward, "A Generalization of the Frechet Distance of Two Curves," *Proceedings of the National Academy of Sciences of the United States of America*, vol. 40, no. 7, pp. 598-602, 1954.
- [28] Z. Danziger, "Discrete Frechet Distance-Mathworks," 5 30 2013. [Online]. Available: <https://in.mathworks.com/matlabcentral/fileexchange/31922-discrete-frechet-distance>.